

Short Communication

## Effect of Duty Cycle on the Corrosion of Mg PEO Coatings

Nasrollah Eslamzadeh<sup>1</sup>, Reza Ebrahimi-Kahrizsangi<sup>1,\*</sup>, saeed Karbasi<sup>2</sup>, Arman Zarebidaki<sup>3</sup>, Farhad Gharavi<sup>4</sup>

<sup>1</sup> Advanced Materials Research Center, Materials Engineering Department, Najafabad Branch, Islamic Azad University, Najafabad, Iran

<sup>2</sup> Department of Biomaterials and Tissue Engineering, School of Advance Technology in Medicine, Isfahan University of Medical Sciences, Isfahan, Iran

<sup>3</sup> Amirkabir University of Technology, Corrosion Engineering and Material Protection Group, Bandar Abbas Campus

<sup>4</sup> Department of Materials Engineering, Sirjan Branch, Islamic Azad University, Sirjan, Iran

\*E-mail: [rezaebrahimi@iaun.ac.ir](mailto:rezaebrahimi@iaun.ac.ir)

Received: 5 December 2017 / Accepted: 4 March 2018 / Published: 5 June 2018

---

Plasma electrolytic oxidation (PEO) is the method of applying corrosion resistant coatings on Mg alloys. Duty cycle is one of the effective parameters on PEO processes that can be employed to investigate the effect of duty cycle on the corrosion behavior. In this study, PEO coatings were fabricated in a silicate electrolyte with duty cycles in the range of 20 to 80%. Phase composition and microstructure of the PEO coatings were analyzed by X-ray diffraction (XRD) and scanning electron microscopy (SEM) followed by energy dispersive spectroscopy (EDS). The corrosion behavior of the PEO coatings was evaluated using potentiodynamic polarization in 3.5 wt.% NaCl solution. According to SEM and polarization results, a decrease in the duty cycle from 60% to 20% was found to result in about 72% reduction in the growth rate of PEO coatings and improvement of the coatings morphology; finally, 94% decrease in corrosion current density was observed.

---

**Keywords:** Mg, Plasma electrolytic oxidation, Oxide coating, Corrosion resistance, Duty cycle

### 1. INTRODUCTION

Magnesium is a light metal with the density of 1.74 gr/cm<sup>3</sup>. It is 1.6 and 4.5 times lighter than aluminum and steel, respectively. High strength to weight ratio, toughness, and good molding capabilities are known as the important properties of magnesium and its alloys, leading to its widespread use in various electrical and electronic, recreational and medical equipment [1-5]. However, the most important limitation is the considerable corrosion rate of magnesium owing to its

active electrochemical potential. Using corrosion-resistant coatings is one way to reduce the corrosion rate of Mg alloys. In comparison to various coating techniques, plasma electrolytic oxidation method has such advantages as fewer environmental risks, cost effectiveness, affordability, and high-speed coverage, making it a popular topic of research [6-10].

During the plasma electrolytic oxidation process occurring at voltages higher than the breakdown voltage, there is the possibility of the discharge phenomenon, leading to plasma creation and the growth of an oxide layer. When electrical discharge occurs, magnesium is melted; as a result, it is flowing through the discharge channels and entering into the coating surface. Subsequently, it is quenched in contact with the electrolyte solution. The layers created by this method have higher stability and adhesion, showing a higher corrosion resistance, as compared to the chemical conversion method. Various parameters including current density, process time, frequency, and duty cycle can influence the oxide coating growth process and corrosion resistance during this process. Extensive research has been conducted regarding the effects of these factors on corrosion behavior [11-16]. Duty cycle, which is among effective parameters on oxide coating growth, is defined as:

$$Dt = \left( \frac{t_{on}}{t_{on} + t_{off}} \right) \times 100$$

, where  $t_{on}$  refer to the on-duration and  $t_{off}$  represents the off-duration during a single cycle [17]. According to this equation, duty cycle is changed with the morphology; the growth rate of PEO oxide coating can be represented, as shown in Figure 1.

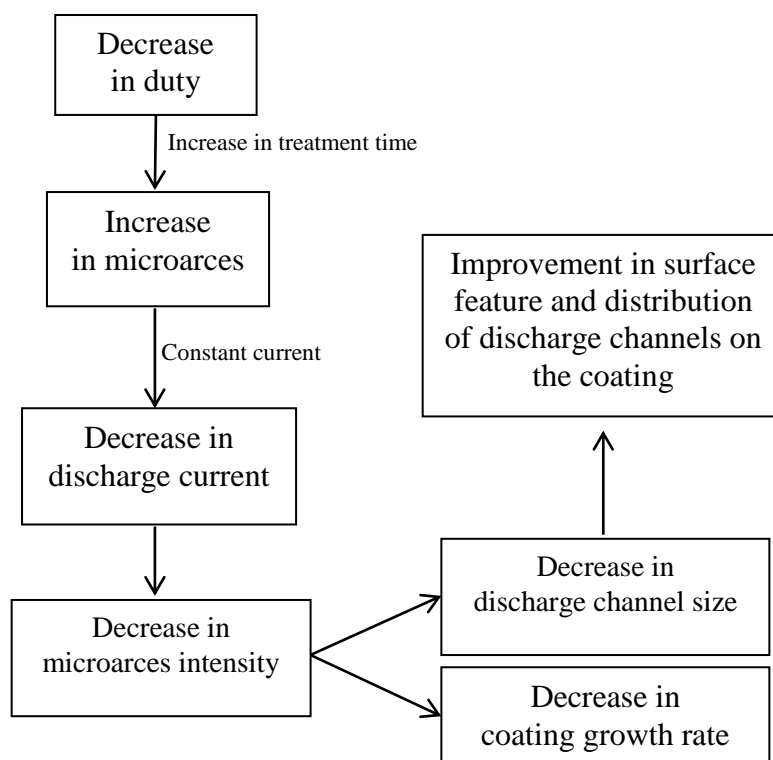


**Figure 1.** Relation between duty cycle and surface morphology of PEO coatings

In a study conducted on AA7075 alloy [18], the use of low-duty cycles increased polarization resistance and adhesion of the coating to the substrate; this was such that the test results of open circuit potential (OCP) were altered in terms of time, showing the higher levels of OCP in the coatings of low duty cycles; this, in turn, verified less susceptibility to corrosion. Also, the analysis of the surface roughness (Ra) of the coatings created in different duty cycles showed that the coatings made in the lower duty cycle had the lowest surface roughness, as well as a smoother coating. In a research that addressed Al6061 alloy [17], it was found that the coatings created in the lower duty cycles had a higher breakdown voltage and higher density sparks, leading to the smoother silicon distribution on the coating surface. Research results on titanium alloy have also shown that the lower duty cycle coating could increase the micro-hardness of the coating [19].

Duty cycle is known as one of the effective parameters of PEO technique that has not been addressed adequately for AZ91 Mg alloys by the researchers. The present research investigated the effect of this parameter on PEO coatings in the case of Mg AZ91 alloy. Also, the surface morphology variation of coatings with duty cycle was illustrated schematically; further, the relation of them with the corrosion behavior of the coatings was investigated.

## 2. MATERIALS AND METHODS

The study used rectangular samples ( $10 \times 10 \times 3 \text{ mm}^3$ ) obtained from AZ91 magnesium alloy (9.05% Al, 0.65% Zn, 0.21% Mn, 0.02% Si, 0.002% Fe, 0.0005% Ni, 0.002% Cu), in the cast ingot form; these served as the substrate. Then, the obtained samples were ground by means of some silicon carbide waterproof abrasive papers up to 1200 grits. Subsequently, the samples were ultrasonically cleaned in acetone and rinsed in distilled water; finally, they were allowed to be dried in warm air. The samples were used as the anode in the PEO process, and some 316 stainless steel sheet having the dimensions of  $40 \times 25 \times 1 \text{ mm}^3$  served as the cathode. By using a power supply of Ruyingaran Sanaat Co. model IRN6000, the current was applied; also, the electrolyte temperature was kept below  $35^\circ\text{C}$  in the coating process.

The oxide coating was created by employing the constant current mode, based on duty cycle changes from 20% to 80%, the current density of  $90 \text{ mA} / \text{Cm}^2$ , the frequency of 100 Hz in a  $0.025 \text{ M Na}_2\text{SiO}_3\text{-}5\text{H}_2\text{O}/0.05 \text{ M KOH}$  electrolyte solution with the  $\text{pH}=12.5$ . For the preparation of this solution, 8.75 ml of  $\text{Na}_2\text{SiO}_3\text{-}5\text{H}_2\text{O}$  in 2000 ml distilled water combined with 3.3 gr KOH and mixed in room temperature for 1 hr. Given that the sample coating conditions could be variable with duty cycle, the samples were encoded with the duty cycle percent of M20 to M80. An attempt was also made to record Voltage variations versus time; in the course of the coating process, the samples were washed with distilled water and after the coating process, they were allowed to be dried by hot air.

X-ray diffraction analysis was carried out by employing a Philips-PW3040 model X-ray diffractometer for the identification of the coating phases. Then, to measure the thickness and study the morphology of the coating at the surface and cross section, a VEGA TESCAN-LMU model SEM scanning electron microscope was used. Due to the insulative nature of the coatings, a thin layer of gold was applied on the surface to create surface conductivity.

Potentiodynamic polarization tests were conducted by employing the Princeton applied (EG & G) model 2273 Potentiostat machine. A conventional three-electrode cell (Flat cell), which consisted of a platinum electrode as the counter electrode, a saturated calomel electrode (SCE) as the reference, and the PEO coatings as the working electrode, was used for all electrochemical measurements; for this purpose, a 3.5% NaCl solution was used at room temperature and after 20 min of the initial delay in order to stabilize the open-circuit potential (OCP). Polarization tests were carried out over a potential range of -250 mV to 1200 mV, based on the OCP, by employing a scan rate of 1 mV/s. Such polarization parameters as corrosion potential ( $E_{\text{corr}}$ ) and corrosion current density ( $i_{\text{corr}}$ ) were obtained from the polarization curves and Tafel analysis in a direct manner. The Stern–Geary equation was also used to measure the linear polarization resistance ( $R_p$ ) of the samples.

### 3. RESULTS AND DISCUSSION

#### 3.1. Fabrication of the oxide film by PEO

In this study, the oxide coating was created using the duty cycles of 20% to 80% to evaluate the influence of the duty cycles on the coating mechanism and the corrosion behavior.

Figure 2 shows voltage variations over time in the samples coated in the silicate electrolyte with the pH of 12.5; also, the current density was 90 mA/Cm<sup>2</sup> and the frequency was 100 Hz in different duty cycles.

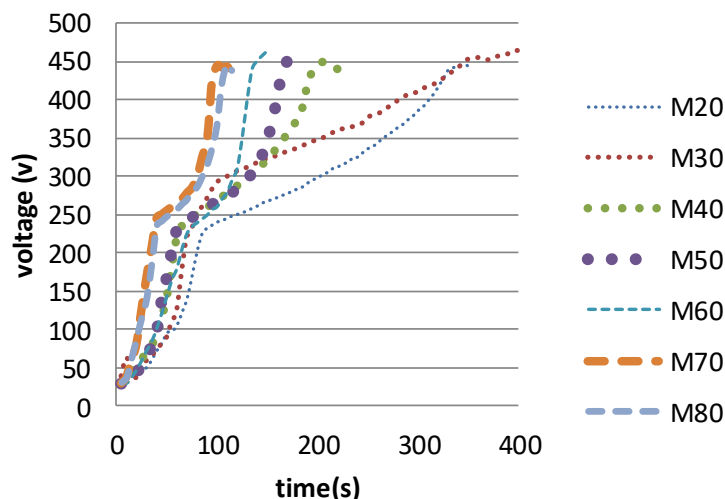


**Figure 2.** Variations of voltage with time for coatings obtained in various duty cycles

According to Fig. 2, voltage was increased at a rapid rate, reaching to the breakdown voltage (approximately 250 V) in the first stage of the coatings growth in different duty cycles. Magnesium dissolution was conducted by reaction 1 at this growth stage, known as anodic oxidation. According to silicate electrolyte solution use, a thin protective layer was developed on the surface during reaction 2. The voltage surge was due to the resistance of this layer against current.

- (1)  $\text{Mg}=\text{Mg}^{2+} + 2\text{e}$   
 (2)  $\text{Mg}^{2+} + \text{SiO}_3^{2-} = \text{MgSiO}_3$

The second stage of the coating growth was after the breakdown voltage began through starting the white sparks on the surface. The initial protective layer disappeared at this stage and during reactions 3 and 4, the first corrosion-resistant oxide layer was formed [20].

- (3)  $\text{Mg}^{2+} + 2(\text{OH}^-) = \text{Mg}(\text{OH})_2$   
 (4)  $\text{Mg}(\text{OH})_2 = \text{MgO} + \text{H}_2\text{O}$

Given the high temperature of plasma process during the oxide layer growth, some forsterite corrosion resistant phase was formed during reactions 5 and 6 by periclase when magnesium silicate was present.

- (5)  $2\text{Mg}^{2+} + \text{SiO}_3^{2-} + 2\text{OH}^- = \text{Mg}_2\text{SiO}_4 + \text{H}_2\text{O}$   
 (6)  $\text{SiO}_2 + 2\text{MgO} = \text{Mg}_2\text{SiO}_4$

Figure 3 shows X-ray diffraction results of the oxide coating surface created during the duty cycle of 20%, with the current density of  $90 \text{ mA} / \text{Cm}^2$  and the frequency of 100 Hz.

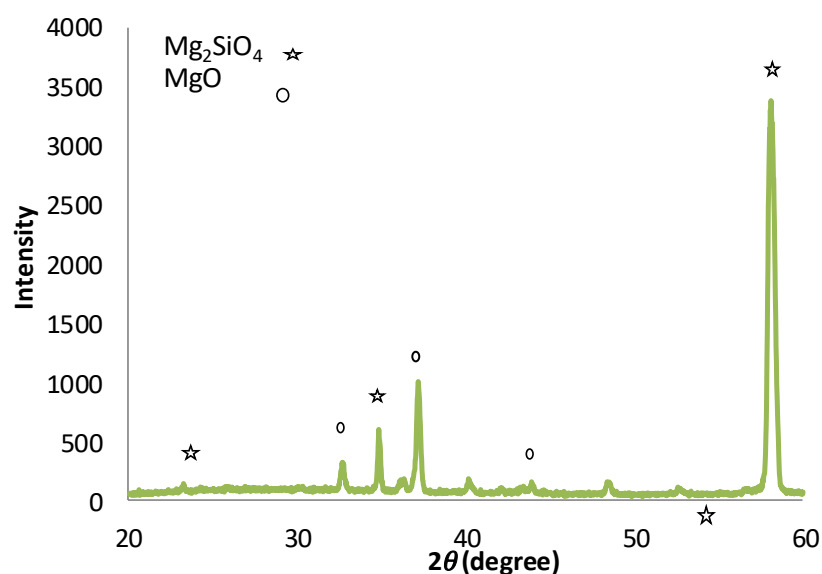


**Figure 3.** XRD patterns of the oxide coating created with 20% duty cycle

The coating surface sparks density and the density of the current discharge channels were reduced over time; the growth of the oxide layer was increased due to coating insulation and its resistance against the current. In the third area of diagram shown in Fig. 2, voltage changes were reduced, and the diagram became smooth when the voltage reached to a maximum value of 450 V. In fact, the sample voltage tended toward sustainability with the development of oxide layer growth through the thick sparks of low-density; the time was considered at the end of the coating process.

According to Fig. 2 and the results obtained by other researchers [11,13,17,21], the diagram tended towards left due to the increased duty cycle, reaching voltage stability in a shorter time; as a result, the coating growth rate could increase. The coating growth rate of the samples M20 and M30

was approximately 0.7 volt / sec in the second stage, and 2.5 volt / sec in the samples M40 to M80. Curves for M20 and M30 samples (Fig. 2) showed the slower growth of the coating, as compared to M40 to M80 samples. According to the duty cycle equation, the applied current time was less for coatings created in the low duty cycle, as compared to those created in the high duty cycle. By considering the constant current and the increased number of spikes on the surface, it could be concluded that the flow rate of each spark was reduced and sparks were formed at a lower intensity level, leading to the reduced size of the discharge channel as well as the reduced growth of the coating; ultimately, the coating smoothness would be increased [17, p.103].

In Figure 4, SEM images of the coatings surface created in the upper and lower duty cycles have been compared. As can be seen, different areas are visible on the PEO coatings, including the cratered structure with a central hole and a nodular structure.

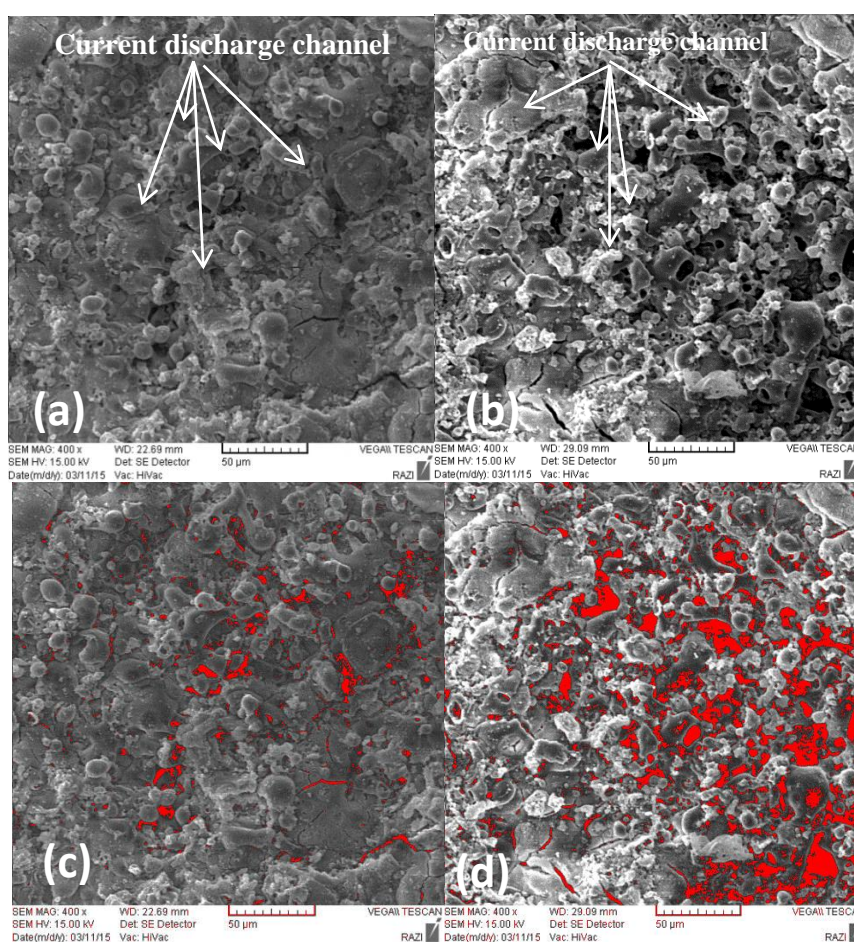


**Figure 4.** Scanning electron micrographs of the surface of coatings obtained with a,c) 20% (M20) and b,d) 60% (M60) duty cycle

The cratered structure with a central hole was found to be the discharge channel; magnesium was melted owing to the high temperature and the strong electric field, flowing through the discharge channel of the substrate / coating intersection towards the coating surface; then it was exposed to the electrolyte and quenched. It is known that the discharge of these channels can have a significant effect

on the growth of the oxide coating [22]. The size and intensity of these areas represent the density and discharge intensity on the surface during coating growth; stronger discharges can lead to the creation of larger cratered regions [23, 24].

According to Fig. 4, the hole size of discharge currents on coatings created in the lower duty cycle was decreased, as compared to those created in the higher duty cycle. The results obtained in other similar studies [17, 25,26] also indicate that using the low duty cycle leads to the increased micro-sparks density on the surface. As a result, more places are created in order to exit the molten magnesium from the substrate towards electrolyte; thus, the time required for coating growth and surface smoothness could be increased. These results were in line with the SEM studies of coatings created in high and low duty cycles. According to the diagrams brought in Fig. 2, the reduced duty cycle led to the enhanced electric field and the increased number of the generated sparks. So, the exit locations of molten magnesium and its freezing could be increased on surface, making the resulting structure smoother.

The schematic of the relationship between duty cycle and discharge channels formed on the PEO coatings is shown in Figure 5.

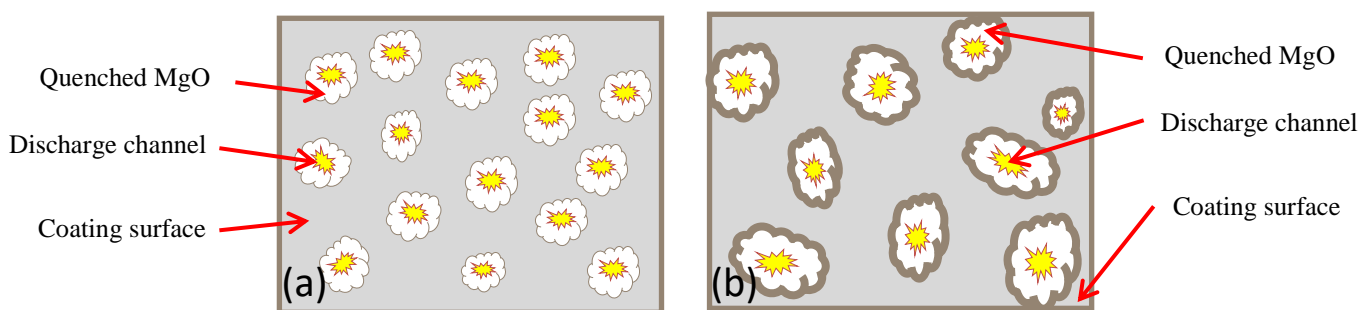


**Figure 5.** Schematic diagrams showing the effect of duty cycle on discharge channels on the surface of PEO coated samples for (a) low duty cycle and (b) high duty cycle conditions

According to this Figure, the increased duty cycles could lead to decreased current discharge locations and electrical discharges with less density and higher intensity. Therefore, current discharge channels that appeared as holes on the coating surface could have bigger dimensions and the coating surface defects would be increased. This difference can be seen in Fig. 4. Therefore, the holes related to discharge channels had higher dimensions; they were developed as defects on the surface of the coating created in the high duty cycle (Fig. 4b), as compared to the one created in the low duty cycle (Fig. 4a). On the other hand, as shown in Figure 4a, discharge channels had higher density and were surrounded by oxide products, creating a smoother surface. Comparing figures 4c and 4d showed that the percentage of the discharge channel was increased from 0.91% in M20 to 9.24% in M60 coating. In a study carried out by Aliofkhazraei and Rouhaghdam [19, p.2096], it was revealed that the smooth oxide layer increased the hardness of the coating and contributed to the smooth distribution of hardness on the surface.

These results agreed with the findings of this study. When the samples were coated, the reduced duty cycle led to ignition on the surface; this, in turn, resulted in the slower, smoother and softer growth of the oxide layer, as well as a high quality coating.

### 3.2. Corrosion properties of the PEO coatings

To compare the corrosion resistance of the PEO samples treated at different duty cycles, Potentiodynamic polarization measurement was employed.

Figure 6 shows the potentiodynamic polarization curves of the bare Mg and the PEO coatings formed in various duty cycles. The obtained results from the polarization test pertaining to the bare Mg and M20 to M80 samples are summarized in Table 1.

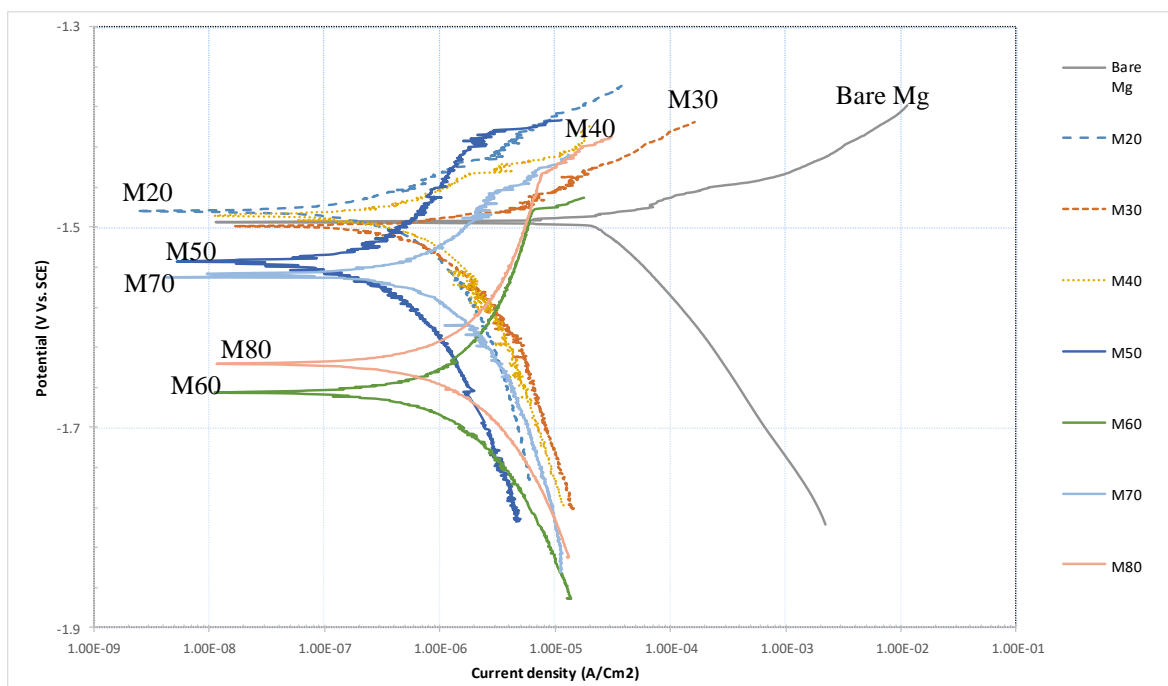


**Figure 6.** Polarization curves of bare Mg and coatings obtained with 20% (M20) to 80% (M80) duty cycle in 3.5% NaCl solution

**Table 1.** Fitting data for M20 to M80 samples.

|         | $i_{corr}$<br>( $\mu\text{A}/\text{cm}^2$ ) | $E_{corr}$<br>(mV Vs SCE) | $R_p \times 10^3$<br>( $\Omega.\text{Cm}^2$ ) | $\beta_a$ (mV/decade) | $\beta_c$ (mV/decade) | MPY   |
|---------|---|---------------------------|---|-----------------------|-----------------------|-------|
| Bare Mg | 21.6  | -1492                     | 0.54  | 34                    | 130                   | 19.42 |
| M20     | 0.21  | -1485                     | 65.4  | 49                    | 89                    | 0.189 |
| M30     | 0.75  | -1495                     | 16.45   | 35                    | 150                   | 0.674 |
| M40     | 0.5   | -1488                     | 32.3  | 54                    | 120                   | 0.449 |
| M50     | 0.59  | -1536                     | 82.4  | 217                   | 231                   | 0.530 |
| M60     | 3.9   | -1667                     | 23.04   | 598                   | 316                   | 3.506 |
| M70     | 1   | -1551                     | 33.09   | 127                   | 190                   | 0.899 |
| M80     | 0.84  | -1638                     | 28.8  | 124                   | 101                   | 0.755 |

As the major parameters of corrosion resistance, the corrosion potentials ( $E_{\text{corr}}$ ), corrosion current densities ( $i_{\text{corr}}$ ), and the relative corrosion rate were obtained from the potentiodynamic polarization plots. Comparing the corrosion current density values in Table 1 indicated that the coatings created by varying amounts of duty cycles had a reduced magnesium corrosion rate, showing the effect of the oxide coating on preventing corrosive ion diffusion into the substrate and its reaction with magnesium. Given that the only variable of these coatings is the duty cycle; the corrosion behavior change of the coatings was dependent on this parameter, to the effect that the corrosion potentials of the coatings created in the lower duty cycle (M20) and the higher duty cycle (M60) were nobler and more active than the corrosion potential of magnesium, respectively. So, it could be inferred that employing the higher values of duty cycle increased the corrosion tendency of the PEO coatings. Also, the corrosion current density was decreased from  $21.6 \mu\text{A}/\text{cm}^2$  in the magnesium alloy to  $3.9 \mu\text{A}/\text{cm}^2$  in M60 and to  $0.21 \mu\text{A}/\text{cm}^2$  in M20. It means that the PEO coating formed in a duty cycle of 60% did not effectively act as a barrier coating. This could be attributed to the uncompact and non-uniform coating which allowed the transfer of  $\text{Cl}^-$  ions from the aggressive solution into the substrate. Chen [27] showed that the increase of the duty cycle from 30 to 50% enhanced the corrosion rate of the PEO coating obtained by the mg alloy. In a study done by Chang et al. [28], it was revealed that when the duty cycle was higher 60%, the porosity of the anodic film was very high, not providing effective protection.

As shown in Table 1, in comparison to the bare Mg, the polarization resistance ( $R_p$ ) was increased and the corrosion current density ( $i_{\text{corr}}$ ) was reduced with the decrease of the duty cycle from 60 to 20%. This showed that the bare Mg had higher susceptibility to corrosion, as opposed to the M20 and the M60 samples. Therefore, the corrosion rate of the PEO coated samples was enhanced with increasing the duty cycle from 20 to 60%.

According to Fig. 2, the increased duty cycle had a significantly directed V-T diagram to the left. In fact, in the first stage of the coating growth and before voltage ignition, both samples showed the same behavior. The coatings created in the lower duty cycle reached a stable voltage of 450 volts in more times during the second stage of coating growth and after ignition. According to the schematic of Fig. 5 and SEM images of Fig. 4, it could be concluded that the created oxide layer had higher balance and stability, as well as higher corrosion resistance, in the M20 coating owing to the longer time needed for the coating growth in the PEO process. The results of SEM can be seen in figure 7, representing the effect of corrosion on the tested coatings surface.

Deep cracks shown in Fig. 7b were related to the coatings created by the 60% duty cycle (M60) after the corrosion test. Meanwhile, the number of cracks of Fig. 7a, which was related to the coatings created by the 20% duty cycle (M20), was decreased on the surface. According to figures 4c and 4d, area of the cracks of coatings after the polarization test was increased from 0.95% in M20 to 5.33% in M60 coating. It showed that the surface of M20 coating was smoother after the corrosion test.

According to the findings of Khan et al. [29], the higher thermal stress and intrinsic stresses have been reported in the coatings created in a higher duty cycle. Wang et al. [30] demonstrated an increase in duty cycle raised the pulse energy; this, in turn could increase the discharge intensity of each spark. It could be inferred that that the rise of discharge intensity could lead to increasing the

temperature of coating; given that it was in contact with the electrolyte and was quenched, the rise of temperature during quenching could lead to the increased thermal stresses.

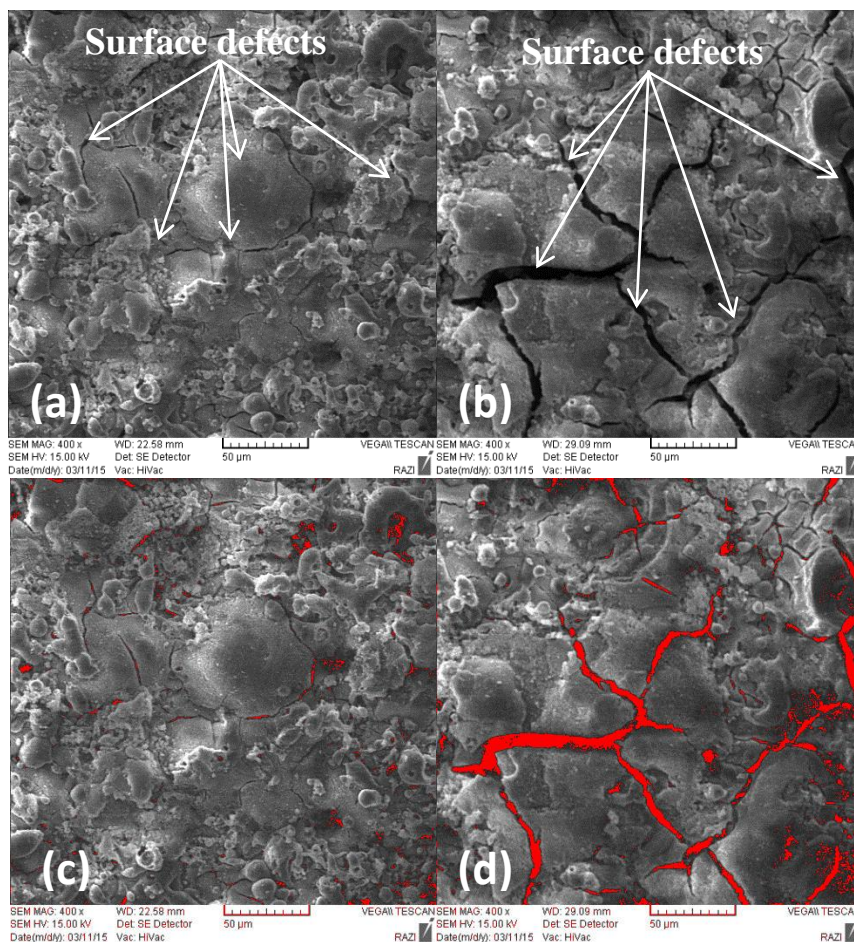


**Figure 7.** Scanning electron micrographs after polarization test of the surface of coatings obtained with a,c) 20% (M20) and b,d) 60% (M60) duty cycle

It is consistent with the observations brought in Fig. 7. the coating defects of the high duty cycle were increased after the corrosion test, as compared to the coating created in the low duty cycle. Intrinsic stresses could be the reason for this difference in the coating behavior. In this case, intrinsic stresses and defects were increased in the M60 coating due to the use of high duty cycle values. So, we could conclude that duty cycle changes from 60% to 20%, as found in this study, led to the improved surface morphology of the coatings and the enhanced coherence and smoothness of the coating surface after the corrosion test; these changes decreased the corrosion current density to 94%.

#### 4. CONCLUSIONS

In the present study, an oxide layer was created on the AZ91 magnesium alloy surface by employing the plasma electrolytic technique with different values of the duty cycle; then, the corrosion behavior of the sample was investigated. The results of this study could be summarized as:

1-A direct relationship was found between the duty cycle percentage and the growth rate of the coating. The increased duty cycle of the coating growth occurring in the second stage with ignition resulted in the rapid growth of coating, reaching the stable voltage.

2-Using the low duty cycle in the PEO coating led to the increased discharge channel density and the reduced intensity of the sparks; consequently, there was a reduction in the corrosion current density of the created coatings, such that the corrosion potential was directed to nobler values upon the improvement of the coating surface morphology.

3-The reduced intrinsic stress of the created oxide coating in the low duty cycle could be regarded as one of the reasons for the reduced corrosion current density of these coatings, as compared to the coatings created in the high duty cycle.

4- It was also found in this study that duty cycle was changed from 60% to 20%; this improved the surface morphology of the coatings increased the coherence and smoothness of the coating surface after the corrosion test; there was also a decrease in the corrosion current density, reaching to 94%.

## References

1. B.L. Mordike, T. Ebert, *Sci. Eng.*, A302 (2001) 37.
2. A. Body, U.T.S. Pillai, B.C. Pai., *J. Indian Foundry*, 57 (2011) 29.
3. M.P. Staiger, A.M. Pietak, J. Huadmai, G. Dias, *Biomaterials*, 27 (2006) 1728.
4. J. J. Zhuang, R. G. Song, N. Xiang, Y. Xiong, Q. Hu, *Surf. Eng.*, 1 (2016) 744.
5. K. C. Tekin, U. Malayoglu, S. Shrestha, *Surf. Eng.*, 6 (2012) 67.
6. N.T. Kirkland, J. Lespagnol, N. Birbilis, M.P. Staiger, *Corros. Sci.*, 52 (2010) 287.
7. K. R. Shin, Y. S. Kim, J. H. Jeong, Y. G. Ko, D. H. Shin, *Surf. Eng.*, 32 (2016) 418.
8. H. Hornberger, S. Virtanen, A.R. Boccaccini, *Acta Biomater.*, 8 (2012) 2442.
9. F. C. Walsh, C. T. J. Low, R. J. K. Wood, K. T. Stevens, J. Archer, A. R. Poeton, A. Ryder, *Surf. Eng.*, 87 (2009) 122.
10. H. M. Wang, Z. H. Chen, L. L. Li, *Surf. Eng.*, 26 (2010) 385.
11. Sh. Lu, B. Lou, Y. Yang, P. Wu, R. Chung, J. Lee, *Thin Solid Films*, 596 (2015) 87.
12. M. Sandhyarani, M. Ashfaq, T. Arunnellaiappan, M. P. Selvan, S. Subramanian, N. Rameshbabu, *Surf. Coat. Technol.*, 269 (2015) 286.
13. Sh. Yu-Long, Y. Feng-Ying, X. Guang-Wen, *Materials Letters*, 59 (2005) 2725.
14. H. Khanmohammadi, S. R. Allahkaram, N. Towhidi, A. M. Rashidfarokhi, *Surf. Eng.*, 32 (2016) 448.
15. A. Ghasemi, N. Scharnagl, C. Blawert, W. Dietzel, K. U. Kainer, *Surf. Eng.*, 26 (2010) 321.
16. Z. P. Yao, D. L. Wang, Q. X. Xia, Y. J. Zhang, Z. H. Jiang, F. P. Wang, *Surf. Eng.*, 28 (2012) 96.
17. V. Dehnavi, B. Luan, D. Shoesmith, X. Y. Liu, S. Rohani, *Surf. Coat. Technol.*, 226 (2013) 100.
18. T. Arunnellaiappan, N. Kishore Babu, L. Rama Krishna, N. Rameshbabu, *Surf. Coat. Technol.*, 280 (2015) 136.
19. M. Aliofkhaezrai, A. Sabour Rouhaghdam, *Applied Surface Science*, 258 (2012) 2093.
20. P. Su, X. Wu, Y. Guo, Z. Jiang, *J. Alloys Compd.*, 773 (2009) 475.
21. Y. Gao, A. L. Yerokhin, E. Parfenov, A. Matthews, *Electrochim. Acta*, 149 (2014) 218.
22. C. S. Dunleavy, I. O. Golosnoy, J. A. Curran, T. W. Clyne, *Surf. Coat. Technol.*, 203 (2009) 3410.
23. R. O. Hussein, D. O. Northwood, X. Nie, J. Vac. *Sci. Technol.*, A28 (2010) 766.
24. R. O. Hussein, X. Nie, D. O. Northwood, A. L. Yerokhin, A. Matthews, *J. Phys. D: Appl. Phys.*, 43 (2010) 105.

25. E. V. Parfenov, A. L. Yerokhin, R. R. Nevyantseva, M. V. Gorbatkov, C. J. Liang, A. Matthews, *Surf. Coat. Technol.*, 269 (2015) 2.
26. V. Dehnavi, B.L. Luan, D.W. Shoesmith, X.Y. Liu, S. Rohani, *Surf. Coat. Technol.*, 226 (2013) 105.
27. J. Chen, W. Zexin, L. Sheng, *Rare Metals*, 31 (2012) 172.
28. L. Chang, C. Fa-he, C. Jing-shun, L. Wen-juan, Z. Zhao, Z. Jian-qing, *Trans. Nonferrous Met. Soc*, 21 (2012) 312.
29. R. H. U. Khan, A. L. Yerokhin, T. Pilkington, A. Leyland, A. Matthews, *Surf. Coat. Technol.*, 200 (2005) 1580.
30. Y.M. Wang, D.C. Jia, L.X. Guo, T.Q. Lei, B.L. Jiang, *Mater. Chem. Phys.*, 90 (2005) 128.

© 2018 The Authors. Published by ESG ([www.electrochemsci.org](http://www.electrochemsci.org)). This article is an open access article distributed under the terms and conditions of the Creative Commons Attribution license (<http://creativecommons.org/licenses/by/4.0/>).